




Predicting the Position of the Internal Landmarks of Middle Cranial Fossa Using the Zygomatic Root: An Attempt to Simplify Its Complexity

Deepika Poonia^{1,*}  Surbhi Wadhwa¹ Anita Mahajan¹ Sabita Mishra¹

¹ Department of Anatomy, Maulana Azad Medical College, New Delhi, India

Address for correspondence Surbhi Wadhwa, MBBS, MD, Department of Anatomy, Maulana Azad Medical College, Room No 233, II Floor, Dean Office Building, Bahadur Shah Zafar Marg, New Delhi -110002, India (e-mail: wadhwa.surbhi@gmail.com).

Indian J Neurosurg 2024;13:119–126.

Abstract

Subtemporal–extradural middle cranial fossa (MCF) surgical approach is used to access pathologies involving anterior or posterior part of the petrous bone or its apex. A reliable and precise identification of the important internal landmarks is key to a safe surgery with decreased incidence of morbidity. The zygomatic root (ZR) serves as a reliable reference guide for the surgeon when navigating through the MCF. The aim of the study is to establish an association between the extent of the ZR to the key internal foramina and bony prominences in lateral fossa of the MCF to help the neurosurgeon to safely navigate through the maze of structures of the MCF. The study demonstrates that the ZR is a reliable marker to estimate and predict the position of foramen ovale, foramen spinosum, and trigeminal fossa but not for the position of hiatus of greater petrosal nerve or the arcuate eminence. Successful localization of the foramen ovale, spinosum, and trigeminal fossa would reduce intraoperative time, ensure lesser retraction of brain, and hence reduce patient morbidity while performing surgeries on lesions of/in the internal acoustic canal, petroclival junctions, cerebellopontine angles, basilar artery, or transovale cannulation for the treatment of trigeminal neuralgia.

Keywords

- ▶ middle cranial fossa approach
- ▶ neuronavigation
- ▶ zygomatic root

Introduction

To access pathologies around the petrous part of the temporal bone that include petrous and petroclival tumors, internal auditory canal (IAC), and posterior cavernous lesions, an extradural–subtemporal middle cranial fossa (MCF) approach to the skull base is often executed. This involves, a temporal bone craniotomy,

careful retraction of temporal lobe and dura to access the petrous bone. The caudal most limit of this standard 4 × 5 (cm) craniotomy incision is the zygomatic arch (ZA).^{1,2} On entry, the surgeon is guided to the target pathology by navigating and using anatomical reference points like the middle meningeal artery that is housed in foramen spinosum (FS), greater petrosal nerve (GPN), which enters the MCF through a hiatus in tegmen tympani; trigeminal ganglion or its mandibular branch of trigeminal nerve, which exits through the foramen ovale (FO); and arcuate eminence (AE), which inconsistently overlies the superior

* Presently working at University College of Medical Sciences, Delhi, India

article published online
June 27, 2022

DOI <https://doi.org/10.1055/s-0042-1750296>.
ISSN 2277-954X.

© 2022. The Author(s).

This is an open access article published by Thieme under the terms of the Creative Commons Attribution-NonDerivative-NonCommercial-License, permitting copying and reproduction so long as the original work is given appropriate credit. Contents may not be used for commercial purposes, or adapted, remixed, transformed or built upon. (<https://creativecommons.org/licenses/by-nc-nd/4.0/>)

Thieme Medical and Scientific Publishers Pvt. Ltd., A-12, 2nd Floor, Sector 2, Noida-201301 UP, India

semicircular canal.^{3,4} The extension of the MCF approach, also, allows access to the posterior cranial fossa to operate on lesions of/in the internal acoustic canal, petroclival junctions, cerebellopontine angles, basilar artery.¹ Thus, a thorough knowledge of the geometry and location of the vital structures present in the MCF is a must.⁵

The ZA is formed by the confluence of the zygomatic process of the temporal bone with the temporal process of the zygomatic bone. The inferior surface of the zygoma or the ZA attaches to the squamous part of the temporal bone by the zygomatic root (ZR) that has an anterior and posterior root converging on the tubercle.⁴ The ZR is an important external landmark that comes in view once the skin is reflected for temporal craniotomy. Routinely, the surgeon does not sacrifice the ZA or its root when accessing the MCF.¹ It thus serves as a reliable reference guide for the surgeon when navigating through the MCF or when locating frontalis branch of facial nerve, inion, transverse sinus, temporal horns of lateral ventricle, temporal tip, and the inferior temporal gyrus.^{1,6}

The newer intraoperative navigation systems have facilitated the identification of the various internal landmarks; however, errors do happen. The aim of the study is to establish an association between the extent of the ZR to the key internal foramina and bony prominences in lateral fossa of the MCF to help the neurosurgeon to safely navigate through the maze of structures of the MCF. The hiatus of GPN, AE, FO, FS, and trigeminal fossa (TF) is laterally projected on the ZR in dry adult skulls. Their linear distances from ZR were measured in the dry skull as well as digital images.

Materials and Methods

The study was performed on 47 dry skulls available in the bone repository of Department of Anatomy, Maulana Azad Medical College, New Delhi. Damaged and chipped bones were excluded from the study. No age or gender records of the bone were available for these skulls. In each skull, initially, the ZR was drawn on the inner table of the lateral skull wall using transillumination technique (→ Fig. 1). The skull was placed in the anatomical position in such a way that the lower margin of the orbit and porion (upper margin of external auditory meatus) was in the same transverse plane (Frankfurt's plane). All skulls were photographed with tripod fixed camera (Sony Cybershot DSC- WX500) positioned directly overhead on the same day to maintain standard conditions. A cut piece of the ruler was placed inside each skull to facilitate calibration of the images (→ Fig. 1). Measurements were performed using ImageJ software available on the internet—<https://imagej.nih.gov/ij/>. Pixel measurement calibration was performed on each image before commencing measurements. Each skull was also measured manually with a digital vernier caliper by an independent observer. An average numerical value of each parameter was recorded.



Fig. 1 Cranial view of the middle cranial fossa (MCF) in a dry skull showing the measurements done. Zygomatic root (ZR) was drawn using transillumination technique on the lateral (L) wall of the MCF. Lateral straight-line projections were drawn and measured on the digital image from the midpoint of foramen ovale (FO), foramen spinosum (FS), trigeminal fossa (TF), hiatus of greater petrosal nerve (GPN), and arcuate eminence (AE). The point of intersection of these on the ZR was noted as a, b, c, d, and e, respectively. The distance of these points (double sided arrows) from anterior root of ZR (aZR,*) was measured along the ZR (solid white line and dashed line is the linear continuation). pZR, posterior root of zygoma.

The parameters measured were length of the ZR, lateral straight-line projection of the midpoint of FO, FS, TF, hiatus of GPN and AE on the inner table of the corresponding lateral wall of the MCF, that is, temporal squama where ZR had been marked. The linear distance of this point from the anterior root of zygoma was also measured (→ Fig. 1). Mean and range of these parameters were calculated. The distribution pattern of the data was tested using Shapiro–Wilk test. The entire length of the ZR was divided into equal thirds and the correlation of the lateral projections of the landmarks to the anterior, middle, and posterior thirds of the ZR was done. Student's paired *t*-test and *p*-value were calculated for left to right comparison. Statistical analysis was done using SPSS version 25.0 (IBM, Armonk, New York, United States).

Results

The length of the ZR was 19.4mm (standard deviation ± 0.36). Shapiro–Wilk test and visual inspection of histograms and box plots showed that the parameters were approximately normally distributed for both left and right sides of the skulls. Paired Student's *t*-test ($p > 0.05$) showed there was no statistically significant difference between the parameters of left and right side (→ Tables 1 and 2). The mean lengths and the range of the lateral straight-line projection of the midpoint of FO, FS, TF, hiatus of GPN and AE on the inner table of the lateral

Table 1 Mean, range, and SD of lateral straight-line projection of various foramina on the length of the ZR in mm. *p*-Value is also shown for left to right comparison

Parameter (mm)	Range (min–max)	Mean ± SD	<i>p</i> -Value
Length of ZR	12.2–28.3	19.4 ± 0.36	0.56
Distance between FO and ZR	12.7–35.1	24.2 ± 0.49	0.56
Distance between FS and ZR	10.2–34.9	21.5 ± 0.41	0.42
Distance between TF and ZR	13.7–44.1	32.5 ± 0.47	0.54
Distance between hiatus of GPN and ZR	12.7–3.44	21.2 ± 0.46	0.81
Distance between arcuate eminence (AE) and ZR	05.4–33.6	18.8 ± 0.54	0.58

Abbreviations: AE, arcuate eminence; FO, foramen ovale; FS, foramen spinosum; GPN, greater petrosal nerve; SD, standard deviation; TF, trigeminal fossa; ZR, zygomatic root.

wall of the MCF, that is, temporal squama, are shown in ►Table 1 (data for all the skulls in ►Table 2). The linear distance of the lateral projection of the various internal landmarks from the anterior root of ZR is depicted in ►Tables 3 and 4 and ►Fig. 2.

The center of FO was projected on the anterior two-third of the length of ZR in 84 specimens (89%) (►Table 5, ►Fig. 2). In two specimens, FO was projected to the anterior root and in two skull sides; the FO did not coincide with the root of zygoma and was present posterior to the posterior root. In contrast, the center of FS was projected on the posterior two-third of the ZR in 79 sides of skull (84%) (►Table 5, ►Fig. 2). The lateral projection of the hiatus of GPN was variable. In 64 specimens (68%), it did not coincide with the ZR and was present posterior to it. It coincided with the ZR in approximately one-third of the total specimens (31%), while in 28 specimens, it coincided with the posterior third of the root, in one specimen with the anterior third, and in one with the middle third (►Table 5, ►Fig. 2). The TF coincided with the ZR in 75 out of 94 specimens and in 78.72% of these it correlated with the posterior two-third of the ZR (►Table 5, ►Fig. 2). The AE did not coincide with the ZR in any specimen (►Table 5, ►Fig. 2).

Discussion

The results show that the while the ZR is a reliable marker to estimate and predict the position of FO, FS, and TF but not for the position of hiatus of GPN or the AE. In 89% of the specimens, FO was projected onto the anterior two-third of the ZR, and FS and TF were projected to the posterior two-third of ZR in 84 and 78.27% specimens, respectively. The hiatus of GPN coincided with the posterior third of the ZR in every one out of three specimens. In none of the specimens did the AE project onto the ZR.

Small structures/openings of MCF are not well visualized by the neuronavigation systems accurately and it is beneficial to use external landmarks like the external auditory canal (EAC) and ZR to predict their locations.^{7,8}

Quick and efficient identification of anatomical landmarks helps to reduce the brain retraction time and the consequent morbidity associated with it. Pathologies often distort the internal anatomy thus necessitating external landmark as an aid for identification.

In the MCF approach, the initial step of dissection requires the surgeon to identify the middle meningeal artery as it exits from the FS, surgeon ligates it and thereafter moves further into the depth of the fossa. Kraysenbühl et al also tried to define to localize the FS in 10 dry skulls using the EAC and ZA, but their results were inconclusive due to large variation. They found the mean distance between the FS- lateral (external) aspect of the arch to be 28mm (23–33) and the distance of this projection from the EAC was 13 mm (range: 10–21mm).⁹ While the depth of the FS from the lateral aspect of the MCF is comparable for Kraysenbühl et al, and Peris Celda at al localized the FS at a depth of 28 and 25.6mm, respectively; we measured this distance to be 21.5mm. Kraysenbühl et al were unable to localize the FS using the ZR due to large variation, and Peris Celda at al concluded that in 86% of cases, the FS was present within ZR width; we found that FS was projected to posterior two-third of ZR in 84% making the ZR a good external landmark to predict its position.

The extradurally located GPN and its hiatus are of utmost importance to the neurosurgeon, who uses it to locate the geniculate ganglion, IAC, or facial nerve or form boundaries of few of the triangles present around the cavernous sinus—Kawase's and Glasscock's.¹⁰ The anatomical plane of GPN is such that its posterior part is shallow in position compared with its anterior portion. This difference in its depth makes it difficult to define its optimum surgical plane. This, along with its small size, predisposes it to traction injury during dural elevation or bone drilling resulting in iatrogenic facial nerve palsy.¹¹ Several researchers, thus, have tried to locate the hiatus of GPN using internal/external landmarks. Tubbs et al found the midpoint of the hiatus was present at a distance of 33 to 45mm from the lateral wall of the MCF. Sennaroglu and Slattery measured this mean distance to be 21.5mm (range: 19.0–24.0mm) and

Table 2 Master chart of the length of lateral straight-line projection (mm) of various internal landmarks on the length of ZR

Right side	1	2	3	4	5	6	7	8	9	10	11	12	13	14	15	16	17	18	19	20	21	22	23
FO	6.4	8.5	10.0	15.7	7.5	5.8	12.5	6.4	7.5	2.5	9.0	2.4	5.3	2.6	8.4	9.5	10.4	6.4	4.5	3.9	9.8	4.9	3.6
FS	14.3	11.8	13.7	19.0	10.9	13.2	13.6	11.9	12.2	8.7	12.6	7.0	33.3	7.7	13.1	13.6	14.7	9.8	9.5	11.3	13.6	11.1	9.4
TF	18.8	13.3	17.7	20.5	15.0	20.2	19.1	15.5	18.7	18.5	19.6	16.9	27.2	12.3	16.5	13.5	18.1	13.7	10.5	15.5	16.3	18.4	10.7
Hiatus for GPN	23.4	21.1	23.9	24.1	17.0	26.7	26.1	29.5	21.2	23.0	24.9	19.1	24.2	20.4	26.4	21.2	22.6	22.3	14.4	30.4	23.7	19.5	18.3
AE	31.8	28.1	30.3	21.2	27.6	39.0	35.3	34.7	39.0	32.4	37.2	35.4	31.1	30.1	38.2	29.8	34.0	31.7	22.9	39.9	30.3	36.4	32.8
Left side	1	2	3	4	5	6	7	8	9	10	11	12	13	14	15	16	17	18	19	20	21	22	23
FO	0.0	10.5	2.9	10.5	8.8	5.9	8.2	7.9	4.5	4.6	2.0	10.3	6.1	0.0	11.0	8.0	8.6	2.4	8.3	2.5	10.2	5.8	0.0
FS	6.7	11.7	7.2	15.1	14.2	10.2	10.7	12.5	9.4	11.1	5.1	15.4	12.0	4.9	16.8	13.5	14.3	7.6	12.2	9.4	13.4	12.9	7.3
TF	14.2	15.8	8.7	16.1	19.0	20.3	19.1	18.2	14.9	18.5	11.8	22.9	17.4	10.8	21.8	12.4	17.4	10.3	14.6	15.5	18.1	20.1	10.5
Hiatus for GPN	18.9	20.3	14.3	20.6	23.8	19.2	21.4	21.8	20.1	27.3	18.8	24.2	24.1	16.5	30.5	22.2	21.5	18.1	18.3	20.7	25.8	19.6	21.3
AE	26.2	26.4	21.6	25.4	35.4	32.1	32.5	33.1	33.9	39.8	31.8	37.0	31.8	26.6	42.4	34.9	42.7	33.1	23.5	30.6	31.4	37.5	30.0

24	25	26	27	28	29	30	31	32	33	34	35	36	37	38	39	40	41	42	43	44	45	46	47
4.8	6.9	9.4	5.0	1.1	6.8	9.7	18.2	8.5	12.5	7.9	8.8	11.6	5.3	7.6	9.3	4.8	8.4	1.4	11.7	4.4	10.5	11.2	5.6
10.3	12.2	12.5	9.0	8.8	12.5	12.5	22.7	13.7	17.5	12.8	16.3	14.8	10.3	11.8	16.3	6.4	12.6	1.9	16.2	6.8	13.2	17.3	12.3
13.8	13.7	15.5	9.8	13.5	13.0	14.9	24.1	12.8	18.8	11.7	14.5	21.2	16.3	15.3	21.1	16.4	16.3	8.2	14.0	8.9	12.8	21.4	18.2
19.4	24.0	21.4	22.6	28.1	24.2	17.3	30.8	26.8	21.5	20.9	19.3	25.5	21.1	19.3	24.1	26.8	24.2	16.3	21.6	11.6	17.0	25.0	20.0
31.6	29.7	29.8	27.2	35.4	32.5	25.8	35.1	33.0	32.5	32.9	27.2	31.7	30.1	30.2	36.2	34.8	31.4	18.5	27.3	25.9	20.1	27.6	31.4
24	25	26	27	28	29	30	31	32	33	34	35	36	37	38	39	40	41	42	43	44	45	46	47
2.7	5.5	8.9	5.6	9.9	24.1	9.3	8.8	10.2	9.5	10.7	7.2	4.2	7.6	6.3	1.6	8.2	18.3	12.1	12.3	3.5	11.1	3.3	1.4
8.0	11.0	15.7	12.6	14.9	4.6	13.2	12.8	13.5	14.6	14.1	12.5	8.4	12.1	11.0	6.1	12.5	22.4	16.4	17.2	8.4	14.4	5.8	8.2
13.5	12.0	14.6	13.4	21.4	7.3	13.9	13.7	13.7	16.1	14.1	14.5	12.0	16.7	16.0	9.9	16.0	20.9	16.2	19.3	9.6	13.8	8.6	12.4
17.8	19.7	28.1	19.8	34.2	14.4	18.4	23.0	22.6	17.5	23.9	22.1	21.9	20.9	22.0	20.0	24.0	27.3	23.4	21.6	20.7	20.5	15.9	24.0
33.2	25.8	30.9	29.0	40.1	27.5	29.4	28.0	32.8	31.0	34.8	27.0	29.7	30.8	31.5	30.0	31.2	32.4	33.3	27.5	27.5	27.5	25.4	26.2

Abbreviations: AE, arcuate eminence; FO, foramen ovale; FS, foramen spinosum; GPN, greater petrosal nerve; TF, trigeminal fossa; ZR, zygomatic root.

Table 3 Distance (mm) of the lateral projection of the internal landmarks from the anterior root of ZR

Parameter (mm)	Range (min-max)	Mean ±SD
FO	00-24.1	07.7 ± 0.43
FS	01.9-33.3	12.3 ± 0.44
TF	07.3-27.2	15.7 ± 0.39
Hiatus of GPN	11.6-34.2	22.1 ± 0.39
AE	18.5-42.7	31.3 ± 0.48

Abbreviations: AE, arcuate eminence; FO, foramen ovale; FS, foramen spinosum; GPN, greater petrosal nerve; SD, standard deviation; TF, trigeminal fossa; ZR, zygomatic root.

22.5 mm (range: 15.0-26.5 mm) in their computed tomography data and anatomical dissections of 10 temporal bones.¹² Their results also show that the anatomic findings and CT images data are consistent. While predicting the location of hiatus of GPN using the ZR, in only one out of three specimens, the hiatus of GPN coincided with the ZR and in these it coincided with the posterior one-third. The hiatus was present at a distance of 21.2 mm (range: 11.6-34.2 mm) from the lateral wall of MCF. We used the posterior (proximal) aspect as our point of measurement as this is closest to the craniotomy incision and most surgeons prefer to dissect the GPN from “posterior to anterior.”¹¹

Most of the studies on FO elucidate its morphology and morphometry. Transovale cannulation for the treatment of trigeminal neuralgia via percutaneous balloon compression, radiofrequency, rhizotomy, and glycerol rhizotomy requires localization of the FO. Despite advancements in technology and methodology, use of navigation systems, fluoroscopy as well as computed tomography localization of FO proves to be difficult in 5.17% of patients due to variations.¹³⁻¹⁵ Failure to successfully cannulate the FO during surgeries results in blindness, brain stem, or temporal hematomas and even death.^{14,15} Thus, localizing the FO is key to successful treatment and management of trigeminal neuralgia. Our observations revealed that in 89% of specimens the FO was located in the anterior two-third of the ZR and was present at a depth of 24 mm from the lateral skull wall. Peris Celda et al found the depth of FO to be 30.1 mm and this lateral projection was within the span of ZR in 86% of cases. This information may further guide the interventional neuroradiologist in localizing it.

On comparison with the western literature available, it is evident that mean depths of the lateral projections are smaller but the distances from the anterior root of the lateral projections are greater in our study. Anthropometrically, the Indian skulls are predominantly dolichocranic, that is, length is greater than the breadth as compared with the Caucasian skulls that are brachyranic, that is, breadth is greater than the length.^{16,17}

Table 4 Master chart of the distance (mm) of the lateral projection of the internal landmarks from the anterior root of ZR

Right side	1	2	3	4	5	6	7	8	9	10	11	12	13	14	15	16	17	18	19	20	21	22	23
Length of ZR	24.6	19.4	23.9	15.7	15.3	23.0	19.2	22.5	28.2	23.3	20.4	23.0	19.0	18.0	21.5	17.9	18.5	18.5	14.4	25.3	17.0	20.6	22.7
Distance between FO-ZR	18.8	22.2	18.3	31.8	22.5	19.1	29.7	21.5	28.3	19.2	21.6	20.1	23.3	14.5	25.9	23.9	21.3	24.9	24.5	26.7	26.4	28.5	29.3
Distance between FS-ZR	17.8	17.4	16.2	28.0	20.4	18.2	25.6	18.4	25.3	18.2	18.6	18.6	19.7	12.7	23.6	20.2	17.8	21.6	21.1	22.6	22.6	24.5	28.7
Distance between TF-ZR	31.2	29.8	27.8	34.5	28.3	33.5	37.6	30.0	40.0	28.1	30.7	37.1	13.7	24.5	36.2	30.0	32.0	32.1	29.2	40.9	31.8	36.5	36.6
Distance between hiatus of GPN-ZR	19.4	16.2	17.0	22.0	19.8	22.6	27.8	16.3	31.4	21.0	20.6	21.8	19.0	17.3	23.5	19.9	19.9	21.3	17.3	25.6	17.3	29.0	23.2
Distance between IAC-ZR	28.2	25.1	22.6	28.4	27.8	34.8	34.8	32.0	40.7	30.9	33.9	34.1	32.9	26.6	35.2	27.6	28.1	30.9	25.0	38.7	32.8	34.3	30.6
Distance between AE-ZR	16.7	13.4	15.8	17.3	18.7	27.6	21.8	20.3	29.5	23.6	18.3	21.1	23.0	17.6	23.4	15.6	17.2	18.5	10.1	25.8	10.4	20.4	23.4
Left side	1	2	3	4	5	6	7	8	9	10	11	12	13	14	15	16	17	18	19	20	21	22	23
Length of ZR	18.8	20.5	14.3	14.2	16.9	20.6	14.6	19.5	22.6	28.0	21.2	27.5	22.8	16.1	19.9	14.7	24.9	21.1	14.7	23.2	14.4	15.8	21.5
Distance between FO-ZR	18.3	22.7	20.3	27.9	22.0	20.3	24.9	21.2	26.0	18.6	18.6	25.2	23.7	12.7	27.3	22.0	20.9	21.8	24.0	17.5	26.5	30.4	26.3
Distance between FS-ZR	18.6	18.7	19.8	26.3	21.2	19.6	22.8	18.0	23.6	19.6	14.8	24.7	21.1	10.2	26.2	19.9	19.9	19.5	19.9	18.2	23.7	26.4	23.8
Distance between TF-ZR	32.8	30.8	27.0	34.7	33.2	34.0	33.2	28.4	33.9	31.8	29.7	40.5	32.8	24.1	38.7	31.7	36.4	31.7	30.0	31.4	34.8	43.3	33.1
Distance between hiatus of GPN-ZR	19.4	12.7	18.7	20.1	24.4	26.8	21.7	18.2	24.6	22.8	19.5	26.0	22.3	12.9	28.0	21.4	23.3	20.4	18.2	20.0	21.6	34.4	23.1
Distance between AE-ZR	18.9	14.9	16.5	18.2	25.4	21.7	18.0	15.7	21.1	28.3	21.8	25.2	17.4	9.2	30.0	24.2	25.1	19.4	11.5	19.8	16.1	29.1	19.3

24	25	26	27	28	29	30	31	32	33	34	35	36	37	38	39	40	41	42	43	44	45	46	47
18.7	20.2	17.0	19.1	25.5	20.4	14.1	18.0	17.8	17.9	17.3	17.2	18.8	14.9	14430.0	19.9	21.7	24.3	16.6	12.2	18.7	16.8	17.3	19.5
28.4	24.5	24.2	28.9	32.0	25.2	23.6	35.1	27.7	31.1	27.6	25.9	22.5	20.5	19.9	21.6	22.5	29.4	27.0	28.0	24.5	21.7	26.9	24.3
22.6	21.6	20.6	25.3	30.8	24.2	18.3	34.9	24.5	27.0	23.6	23.6	19.5	18.6	16.2	22.2	14.8	25.9	23.2	25.0	20.2	16.1	24.4	21.4
34.6	29.4	31.0	34.9	42.3	31.8	23.9	44.1	33.5	38.5	34.4	32.8	31.0	20.0	27.3	34.3	30.9	36.7	34.3	34.6	30.1	27.8	37.7	32.6
23.5	15.9	16.3	16.9	26.2	19.8	13.0	34.0	18.3	28.1	23.0	22.2	17.3	15.9	14.3	21.5	18.6	27.1	23.4	26.7	23.9	17.0	27.0	19.2
32.3	32.5	33.1	45.2	43.6	39.1	22.5	50.6	32.0	41.1	31.9	35.9	31.4	32.7	30.0	37.7	35.4	41.5	35.0	37.2	25.9	21.5	39.3	18.2
19.5	16.7	14.2	20.8	27.6	21.6	5.4	33.6	16.5	17.9	15.2	18.0	15.4	11.8	11.1	21.2	14.2	24.1	13.8	25.7	17.0	8.4	12.6	19.5
24	25	26	27	28	29	30	31	32	33	34	35	36	37	38	39	40	41	42	43	44	45	46	47
19.8	17.9	15.9	16.5	28.3	14.7	24.8	17.3	16.8	18.4	17.5	17.0	16.1	15.9	23.4	18.8	24.5	22.0	24.2	19.6	20.0	20.5	20.9	16.3
22.7	22.5	24.0	24.7	29.0	0.0	18.0	25.6	19.7	27.9	20.9	22.9	16.2	22.1	18.9	18.0	29.4	30.9	27.3	31.3	26.5	27.2	22.9	30.7
19.7	20.1	24.9	24.1	26.3	22.5	21.9	24.1	16.4	23.6	17.4	20.5	15.4	19.9	16.3	13.8	26.0	24.5	23.9	28.7	23.2	23.9	20.1	26.2
28.7	26.7	30.3	34.2	40.0	31.0	33.2	32.4	28.7	36.2	30.6	31.9	28.6	31.5	31.1	25.1	35.7	37.5	35.2	38.1	32.8	32.8	29.9	34.1
18.8	12.9	26.3	17.4	20.8	23.1	28.6	17.7	16.9	26.5	17.7	17.8	17.8	19.3	15.9	13.5	27.0	14.6	23.2	24.4	24.5	25.3	20.6	22.9
14.2	10.8	23.7	24.2	24.6	21.9	17.6	18.8	8.9	22.6	10.1	17.3	12.9	19.7	16.4	11.0	24.2	20.3	16.3	22.5	21.1	16.0	21.8	17.1

Abbreviations: AE, arcuate eminence; FO, foramen ovale; FS, foramen spinosum; GPN, greater petrosal nerve; IAC, internal auditory canal; TF, trigeminal fossa; ZR, zygomatic root.

Table 5 Number distribution of localization of FO, FS, TF, hiatus for GPN and AE with respect to the anterior, middle, and posterior third of root of zygoma

Landmark	Coincide with ZR	Not coincide	Anterior third	Middle third	Posterior third	Posterior to root of zygoma
FO	92	2	38	46	8	2
FS	87	7	8	44	35	7
TF	75	19	1	17	57	19
Hiatus for GPN	30	64	1	1	28	64
AE	1	94	1	0	0	94

Abbreviations: AE, arcuate eminence; FO, foramen ovale; FS, foramen spinosum; GPN, greater petrosal nerve; TF, trigeminal fossa.

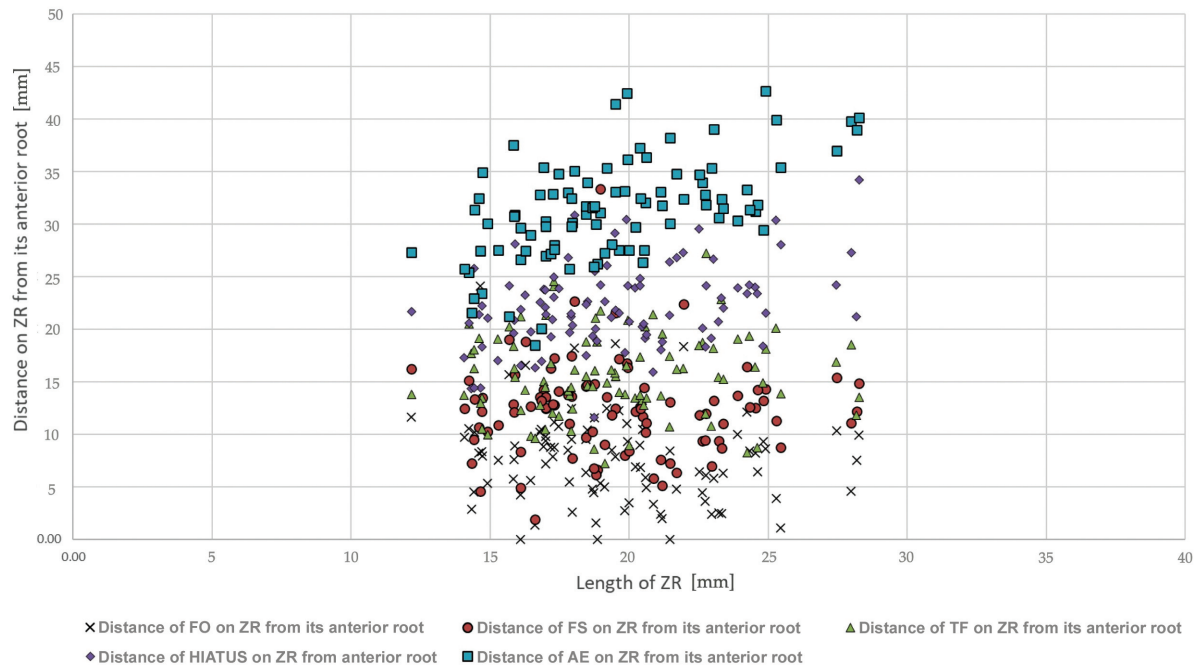


Fig. 2 Scatter plot displays the distribution of the various foramina and their correlation with the length of the zygomatic root (ZR) in mm. AE, arcuate eminence; FO, foramen ovale; FS, foramen spinosum; TF, trigeminal fossa.

Limitation of This Study

Due to the small sample size and lack of gender data, we were unable to study laterality and sex differences between the parameters. Also, the demographic data of the skull was unavailable. Future studies with larger sample size with skulls of known demography and gender would be helpful.

Conclusion

The ZR is a reliable landmark to predict the position of FO, FS, and TF in approximately 80% of patients and the hiatus of GPN in one out of three patients. Its use with the newer neuronavigational systems would help the surgeon to successfully localize the FS, FO, and TF and even hiatus of GPN. This can potentially reduce intraoperative time, lesser brain retraction and potentially can reduce patient operative morbidity.

Conflict of Interest

None declared.

References

- Dayoub H, Schueler WB, Shakir H, Kimmell KT, Sincoff EH. The relationship between the zygomatic arch and the floor of the middle cranial fossa: a radiographic study. *Neurosurgery* 2010;66 (6, Suppl Operative):363–369
- Zanoletti E, Martini A, Emanuelli E, Mazzoni A. Lateral approaches to the skull base. *Acta Otorhinolaryngol Ital* 2012;32(05): 281–287
- Maina R, Ducati A, Lanzino G. The middle cranial fossa: morphometric study and surgical considerations. *Skull Base* 2007;17(06):395–403
- Standring S. *Gray's Anatomy: The Anatomical Basis of Clinical Practice*. 42nd edition. London: Elsevier; 2020: 560–563
- Djalilian HR, Thakkar KH, Hamidi S, Benson AG, Mafee MF. A study of middle cranial fossa anatomy and anatomic variations. *Ear Nose Throat J* 2007;86(08):474–481, 476–481
- Beckman JM, Vale FL. Using the zygomatic root as a reference point in temporal lobe surgery. *Acta Neurochir (Wien)* 2013;155 (12):2287–2291
- Komune N, Matsushima K, Matsuo S, Safavi-Abbasi S, Matsumoto N, Rhoton AL Jr. The accuracy of an electromagnetic navigation system in lateral skull base approaches. *Laryngoscope* 2017;127 (02):450–459
- Peris Celda M, Perry A, Carlstorm LP, Graffeo CS, Driscoll CLW, Link MJ. Key anatomical landmarks for middle fossa surgery: a surgical anatomy study. *J Neurosurg* 2019;131: 1561–1570
- Krayenbühl N, Isolan GR, Al-Mefty O. The foramen spinosum: a landmark in middle fossa surgery. *Neurosurg Rev* 2008;31(04): 397–401, discussion 401–402
- Tubbs RS, Custis JW, Salter EG, Sheetz J, Zehren SJ, Oakes WJ. Landmarks for the greater petrosal nerve. *Clin Anat* 2005;18(03): 210–214
- Jittapiromsak P, Sabuncuoglu H, Deshmukh P, Nakaji P, Spetzler RF, Preul MC. Greater superficial petrosal nerve dissection: back to front or front to back? *Neurosurgery* 2009;64(5, Suppl 2): 253–258, discussion 258–259
- Sennaroglu L, Slattery WH III. Petrous anatomy for middle fossa approach. *Laryngoscope* 2003;113(02):332–342
- Georgiopoulos M, Ellul J, Chroni E, Constantoyannis C. Minimizing technical failure of percutaneous balloon compression for trigeminal neuralgia using neuronavigation. *ISRN Neurol* 2014; 2014:630418

- 14 Zdilla MJ, Hatfield SA, McLean KA, Cyrus LM, Laslo JM, Lambert HW. Circularity, solidity, axes of a best fit ellipse, aspect ratio, and roundness of the foramen ovale: a morphometric analysis with neurosurgical considerations. *J Craniofac Surg* 2016;27(01):222-228
- 15 Zdilla MJ, Hatfield SA, Mangus KR. The angular relationship between the foramen ovale and the trigeminal impression: percutaneous cannulation trajectories for trigeminal neuralgia. *J Craniofac Surg* 2016;27(08):2177-2180
- 16 Ilayperuma I. Evaluation of cephalic indices: a clue for racial and sex diversity. *Int J Morphol* 2011;29:112-117
- 17 Khanduri S, Malik S, Khan N, et al. Establishment of Cephalic Index using cranial parameters in a sampled north Indian population. *Cureus* 2021;13(06):e15421